Am J Physiol Cell Physiol 295: C1399–C1408, 2008.
First published September 24, 2008; doi:10.1152/ajpcell.00342.2008.

Impact of overexpression of metallothionein-1 on cell cycle progression and zinc toxicity

Paul J. Smith,[1] Marie Wiltshire,[1] Emeline Furon,[1] John H. Beattie,[3] and Rachel J. Errington[2]

Departments of [1]Pathology and [2]Medical Biochemistry, School of Medicine, Cardiff University, Cardiff; and [3]Rowett Research Institute, Aberdeen, Scotland, United Kingdom

Submitted 2 July 2008; accepted in final form 17 September 2008

Smith PJ, Wiltshire M, Furon E, Beattie JH, Errington RJ. Impact of overexpression of metallothionein-1 on cell cycle progression and zinc toxicity. *Am J Physiol Cell Physiol* 295: C1399–C1408, 2008. First published September 24, 2008; doi:10.1152/ajpcell.00342.2008.—Metallothioneins (MTs) have an important role in zinc homeostasis and may counteract the impact of oversupply. Both intracellular zinc and MT expression have been implicated in proliferation control and resistance to cellular stress, although the interdependency is unclear. The study addresses the consequences of a steady-state overexpression of MT-1 for intracellular zinc levels, cell cycle progression, and protection from zinc toxicity using a panel of cell lines with differential expression of MT-1. The panel comprised parental Chinese hamster ovary-K1 cells with low endogenous expression of MT and transfectants with enhanced expression of mouse MT-1 on an autonomously replicating expression vector with a noninducible promoter. Cell cycle progression, determined by flow cytometry and time-lapse microscopy, revealed that enhanced cytoplasmic expression of MT-1 does not impact on normal cell cycle operation, suggesting that basal levels of MT-1 expression are not limiting for background levels of oxidative stress. MT-1 overexpression correlated with a steady-state increase in cytoplasmic free Zn^{2+}, assessed using the fluorescent zinc-sensor Zinquin, particularly at high levels of overexpression, further suggesting that zinc availability is normally not limiting for cell cycle progression. Enhanced MT-1 expression, over a 10-fold range, had a clear impact on resistance to Cd^{2+} and Zn^{2+} toxicity. In the case of Zn^{2+}, the degree of protection afforded was less, indicating that MT-1 has a limited range and saturable capacity for effecting resistance. The results have implications for the use of cellular stress responses to exogenously supplied zinc and zinc-based systemic therapies.

cadmium; metallothioneins; flow cytometry; two-photon laser scanning microscopy; Zinquin

ZINC IS AN ESSENTIAL TRACE element with roles in growth and development, as well as in immune function (53). Zn^{2+} ions are critical components of multiple regulatory proteins and are, therefore, subject to homeostatic control at the cellular level (53). Intracellular free zinc concentrations can show transient increases in cells responding to genotoxic and nitrosative stress conditions (27, 44, 54). High levels of free intracellular zinc are potentially cytotoxic, and protection is afforded by a coordinated regulation of transport, storage, and trafficking pathways (6, 39). Important pathway components include zinc transporter families and metallothioneins (MTs). MTs play a role in both zinc and copper homeostasis and comprise a class of ubiquitously occurring low-molecular-weight cysteine- and metal-rich proteins, containing conserved sulfur-based metal clusters, with diverse functions, including potentially protective effects against oxidative stress and highly toxic metals, such as cadmium (32). Computational models for Zn^{2+} homeostasis in cultured cortical neurons suggest that intracellular free Zn^{2+} transients and total Zn^{2+} content observed require high-affinity cytosolic metal binding moieties in addition to MTs (9). Thus the impact of MT overexpression on normal growth control or protection from zinc toxicity would appear to be complex (36). Understanding the interplay between zinc-induced stress responses and MT expression is relevant to a current rationale for the use of a managed supply of zinc in providing safer anticancer therapies (49, 51). Here we have focused on the role of the innate expression of MT on cell proliferation, protection from zinc toxicity, and the steady-state levels of available intracellular Zn^{2+} (37).

The metal ions, for which MT has a high affinity, are zinc, copper, cadmium, and mercury (26, 48). Cadmium is cytotoxic, and its compounds are weak mutagens and clastogens (5). Mice deficient in MT were found to be more susceptible to cadmium (20), supporting it having a function in heavy metal detoxification. However, it is becoming increasingly clear that a major function of MT may involve biologically relevant metals, primarily zinc and copper (45). Due to the widespread distribution of MTs and their highly conserved structure, it has been suggested that trace metal homeostasis and metabolism may be important roles for MTs (3, 45). MT has four isoforms (MT-I to MT-IV). The two main isoforms, MT-I and MT-II, are expressed in almost all mammalian tissues (18). They are generally expressed at basal levels, while being inducible by a number of factors, such as metals, hormones, inflammatory cytokines, and xenobiotics (17). While both mice and humans contain MTs in their tissues, the genes coding for them differ. Mice have four MT genes, one for each isoform (23, 36), whereas humans have at least 16 MT genes. Of the four mouse MT genes, the MT-1 and MT-2 genes are expressed in almost all organs in any stage of development. Seven different genes in humans encode MT-I (13, 16). Human MT-IE and MT-IA levels are increased with Cd^{2+}, Zn^{2+}, or Cu^{2+} pretreatment (13). Metal-responsive elements are necessary for heavy metal-induced transcription, and metal-responsive elements are associated with human MT-IIA and mouse MT-I genes (21).

The most widely expressed mammalian MT-1 and MT-2 isoforms are rapidly induced in the liver by a wide range of metals, drugs, and inflammatory mediators (10). The roles of the MT-1/MT-2 isoforms in zinc homeostasis, protection against heavy metal toxicity, and oxidative damage are related

Address for reprint requests and other correspondence: P. J. Smith, Dept. of Pathology (Tenovus Bldg.), School of Medicine, Cardiff Univ., Heath Park, Cardiff CF14 4XN, UK (e-mail: smithpj2@cf.ac.uk).

The costs of publication of this article were defrayed in part by the payment of page charges. The article must therefore be hereby marked "*advertisement*" in accordance with 18 U.S.C. Section 1734 solely to indicate this fact.

to their cluster integrity (50). Although detoxification of heavy metals seems to be a property of MTs, it may not be their primary function. Cells with lower levels of MT are more sensitive to DNA damage, while overexpression of MT appears to reduce spontaneous mutagenesis rates (31). MT may also play a particular role as an antioxidant in the nucleus, and hence intracellular MT location at sensitive phases of the cell cycle may be critical in supporting stress responses. MTs are thought to store and release metals, such as zinc and copper, to allow low intracellular concentrations of them to be maintained within homeostatic levels for zinc-requiring proteins without triggering toxicity responses (36). MTs are not thought to be particularly important in protecting against zinc or copper toxicity, since efflux systems may fulfill this role. However, cells and mice lacking MT-I and MT-II are slightly more susceptible to zinc toxicity (36). Here we have sought to explore the relationship between enforced MT-1 overexpression, protein location assessed by confocal microscopy, dynamics of cell cycle progression using DNA content and high-resolution time lapse imaging, the homeostasis of intracellular free zinc assessed by flow cytometry, and the tolerance of toxic levels of exogenously supplied Zn^{2+}.

Using a derivative of the Chinese hamster ovary (CHO)-K1 cell line (19) that shows stable overexpression of MT, it was previously found that, while MT overexpression protects against cadmium toxicity, it has no influence on mercury, staurosporine, or hydrogen peroxide toxicity. This previous study (4) used an autonomously replicating expression vector to transfect CHO-K1 cells, chosen because of their low endogenous expression of MT, even after treatment with metals. The pBPV vector, with a noninducible promoter, has been used to generate transfectants that overexpressed MT to obtain an induction-independent evaluation of MT protection against exogenously supplied Zn^{2+}, using Cd^{2+} as a reference (4). Furthermore, we have established stable subclones of a MT-1 high-expressing transfectant, to reduce the potential heterogeneity in MT expression and to provide a finer analysis of the impact of different levels of MT-1 expression on Zn^{2+} homeostasis and tolerance. The results suggest that enhanced cytoplasmic expression of MT-1 does not impact on normal cell cycle operation but was related to an increase in the basal levels of intracellular free Zn^{2+}. Here we have defined labile or free Zn^{2+} as that available to the fluorescent zinc-sensor Zinquin (61). Enhanced MT-1 expression, over a 10-fold range, had a clear impact on both cadmium and Zn^{2+} toxicity, although, in the case of Zn^{2+}, the degree of protection afforded was far less.

MATERIALS AND METHODS

Cell lines and culture. The mouse MT-1 (mMT-1)-overexpressing cell lines were produced at the Rowett Research Institute (4). Briefly, genomic DNA encompassing the complete coding sequence of the mMT-1 gene (+65 to +1240) was inserted into the pBPV expression vector (Pharmacia Biotech, St. Albans, UK) downstream of an mMT-1 gene promoter. Upstream of this promoter is the Moloney murine sarcoma viral enhancer, which is reported to suppress inducibility of the mMT-1 promoter by metals and other factors, and at the same time drive the overexpression of the inserted gene. The pBPV vector with a noninducible promoter was used to give stable overexpression of MT, providing an induction-independent evaluation of resistance associated with MT (4). The CHO-K1 cell line has epithelial morphology and is a subclone of the parental CHO cell line, which was derived from the ovary of an adult Chinese hamster (19). CHO-K1 cells show low-endogenous expression of MT due to MT gene methylation (24). CHO-K1 cells were transfected with the plasmid construct using lipofectin, and stably transfected clones that overexpressed mMT-1 were selected according to their resistance to cadmium. Several cadmium-resistant clones were isolated, and their MT expression was characterized by radioimmunoassay (52). The endogenous antioxidant status of these cells was also characterized (52), and clones showing similar levels of glutathione peroxidase, catalase, superoxide dismutase, and reduced glutathione, but distinct levels of mMT-1 overexpression, were selected for further study. Following removal of first passage cells from liquid nitrogen, single layer cultures of the clones and wild-type CHO-K1 cells were maintained in Eagle's minimum essential medium (Sigma) supplemented with 10% fetal calf serum, 2 mM glutamine, 100 IU penicillin/ml, and 100 mg streptomycin/ml. The cultures were incubated at 37°C, in an atmosphere of 5% CO_2 in air. The cells were routinely detached with trypsin EDTA, split, and resuspended.

Reagents. Zinquin ethyl ester {Zinquin E, [2-methyl-8-(4-methylphenylsulfonylamino) quinolinyl] oxyacetic acid ethyl ester} was purchased from Alexis and stored as a 5 mM stock solution in ethanol at 4°C (61, 62). E9 antibody, sourced from DAKO (Cambridge, UK) and donated by B. Jasani (Cardiff University), was used to detect MT, having been shown previously to be specific to MT (26). Mouse immunoglobulin G was used as a negative control. Goat anti-mouse FITC was the secondary antibody to allow indirect immunofluorescence. Cadmium sulfate (Sigma) was made up to provide a 10 mM Cd^{2+} stock solution. Zinc sulfate (BDH Chemicals) was made up to provide a 200 mM Zn^{2+} stock solution. Both solutions were filter sterilized before initial use and storage.

Clonogenic survival assay. Cells were plated at 300 cells/well of standard six-well culture plates and allowed to attach for 6 h under normal culture conditions before the direct addition of concentrated stock solutions of $ZnSO_4$ to yield the required Zn^{2+} concentration (or Cd^{2+} in the case of cultures treated with $CdCl_2$). Cultures were incubated for a further 6 days to permit colony formation before washing twice with phosphate-buffered saline (PBS) and fixation in 70% ethanol, at room temperature. After removal of ethanol, cells were left to air dry overnight. Cells were stained by 10% "Gurrs"-improved R66 Giemsa solution for 10–15 min, before being washed with water and air drying. The number of colonies was counted, and surviving fractions calculated.

Cell cycle analysis and laser light scatter. Cell cycle analysis of Triton X-100 permeabilized cells, and ethidium bromide stained nuclei was performed, as described previously (43).

Time-lapse microscopy: acquisition and analysis. CHO-K1 and CHO-K1 MT-1 2.20 cultures were established in multiwell dishes and transferred to a time-lapse instrument (28, 29) designed to capture transmission-phase images from multiwell plates. The Axiovert 100 microscope (Carl Zeiss, Welwyn Garden City, UK) was fitted with an incubator to maintain 37°C/5% CO_2 (Solent Scientific, Portsmouth, UK), and images were captured using an ORCA-ER charge-coupled device camera (Hamamatsu, Reading, UK). Illumination was controlled by a shutter in front of the transmission lamp, and an *x*,*y*-positioning stage with separate *z*-focus (Prior Scientific, Cambridge, UK) controlled multifield acquisition. Image capture was controlled by AQM 2000 software (Kinetic Imaging). All images were collected with a ×10 (PH1) apochromat objective lens, providing a field size of 500 × 500 μm. Sequences were captured over an extended incubation period every 10 min and multiple fields. The analysis of the images was performed with the integrated AQM 2000 software package (Kinetic Imaging, Nottingham, UK). Each cell in the field was tracked, and the time to event and duration recorded. The time-lapse event curves were processed and analyzed as previously described (28, 29) for rodent cells.

Immunoblotting. Approximately 2×10^6 cells were pelleted by centrifugation at 1,250 *g* for 5 min, washed once with ice-cold PBS, and lysed with 100 μl of sample loading buffer (44). The method for 12% SDS-polyacrylamide gel protein separation has been described previously (44). Antibodies used were diluted in wash buffer (100 mM Tris, pH 7.5, 0.9% wt/vol NaCl, and 0.1% Tween 20) and comprised anti-MT-1 E9 antibody used at 1:50 dilution; membranes were washed and incubated with appropriate dilutions (1:2,000–1:5,000) of horseradish peroxidase-linked secondary antibody (Amersham) at room temperature for 1 h. Immune complexes were detected by enhanced chemiluminescence detection (ECL kit; Amersham Biosciences, Amersham, UK).

Immunofluorescence. Cells were washed twice in PBS, before fixation with 2 ml of 2% paraformaldehyde/0.1% Triton added to each well and left overnight in the fridge at 4°C. The following day, cells were washed twice with PBS, then blocked by 1 ml of 2% horse serum/0.5% bovine serum albumin (BSA) PBS being added to each well for 30 min, at room temperature. After washing twice with PBS, coverslips were removed from the wells and placed in 10-cm dishes. Two hundred microliters of E9 antibody in 0.5% BSA/PBS were added to the remaining coverslips at a final concentration of 8 g/ml. Two hundred microliters of mouse immunoglobulin G in 0.5% BSA/PBS were added to the remaining coverslips at a matched concentration. After being left overnight at 4°C, coverslips were washed twice with PBS, and FITC was then added at a 1:75 or 1:100 dilution in 0.5% BSA/PBS, followed by incubation at 37°C, in air with 5% CO_2, for 1 h. After coverslips were washed twice in PBS, coverslips were mounted on slides with Vectashield (Vector Laboratories) before imaging by laser scanning microscopy (42).

Analysis of Zinquin-Zn^{2+} by flow cytometry. Following experimental manipulations cells were analyzed immediately using a FACS Vantage flow cytometer (Becton Dickinson Immunocytometry Systems, San Jose, CA) incorporating an Innova Enterprise II argon ion laser (Coherent, Santa Clara, CA) emitting 488 nm and multiline UV (351–355 nm; 30 mW) wavelengths, as described previously (44). Forward scatter (master signal) and side scatter were acquired in linear mode for 10,000 cells. Zinquin fluorescence (350- to 360-nm excitation wavelength range; 485-nm maximum emission wavelength) originating from the multiline ultraviolet laser excitation was collected in linear mode at a photomultiplier position protected by a DF 424/44-nm and 510-nm dichroic filters. CELLQuest software (Becton Dickinson Immunocytometry Systems) was used for signal acquisition and analysis. Data are expressed as mean fluorescence intensity for populations of intact single cells calculated using CELLQuest software.

Analysis of Zinquin-Zn^{2+} by two-photon excitation laser scanning microscopy. Cells were treated and loaded with Zinquin-E and analyzed as described previously (41, 44). These preparations were placed onto Labtek chambered coverglass (NUNC catalog no. 178565) and mounted onto an inverted microscope (Zeiss Axiovert 100). Three-dimensional (*x*, *y*, *z*) images were acquired through the cells using a laser scanning microscope with two-photon excitation (BioRad 1024MP, BioRad Microscience, Hemel Hempstead, UK). Two-photon excitation (by which infrared wavelength light can be used to elicit fluorescence from a UV-excitable fluorochrome) was achieved using a mode-locked 10-fs pulsed Titanium-Sapphire laser (Verdi-Mira 900, Coherent Lasers, Cambridge, UK) tuned to 780 nm; fluorescence emission was acquired between 460 and 650 nm. All experiments were conducted using a ×60, 1.4 numerical aperture oil immersion objective lens. For visualization, the entire three-dimensional image was also projected using a maximum intensity algorithm into a single two-dimensional view using the standard analysis software (LaserSharp version 3.0, BioRad Microscience).

RESULTS

MT-1 expression and Cd^{2+} toxicity. Parental CHO-K1 and MT-1 transfectant clones were assessed for clonogenic potential under continuous exposure to Cd^{2+} (Fig. 1*A*), and the results compared with steady-state levels of MT-1 expression (Fig. 1*B*). The results reveal low (up to 10-fold; clone 1.30.1), moderate (>10-fold; clone 1.5.1), and high (>100-fold; clone 2.20.1) levels of clone resistance to Cd^{2+}, comparing 50% inhibition concentration (IC) values with the corresponding value for parental CHO-K1 cells (<200 nM Cd^{2+}). The resistance pattern is mirrored by the MT-1 expression for clones 1.5.1 and 2.20.1. The low and barely detectable level of enhanced MT-1 expression in clone 1.30.1 (confirmed by radioimmunoassay; J. H. Beattie, unpublished data) was associated with the lowest but significant level of Cd^{2+} resistance. Growth curves for CHO-K1 and the 2.20.1 transfectant in the presence of Zn^{2+} were analyzed to determine the rapidity for engaging complete growth inhibition. The results indicate the restricted range (125–500 μM Zn^{2+}; Fig. 1*C*) for subtoxic vs. rapid and complete growth inhibition for both CHO-K1 cells and the MT-1 transfectant. Using a comparison concentration of 300 μM Zn^{2+}, the three transfectant clones showed Zn^{2+} resistance patterns that ranked the same as for Cd^{2+} (Fig. 1*D*).

MT-1 expression and cell cycle dynamics. CHO-K1 cells and the high-expressing MT-1 transfectant clone 2.20.1 were compared for their cell cycle dynamics at the highest resolution using individual cell time lapse imaging to determine the frequency, nature, and duration of morphologically discernible cell cycle events (namely a completed mitosis, a failed mitosis generating polyploidy cells, an abnormal division resulting in 3 or 4 daughter cells, a cell death). Tracking such cell events also reveals the prevalence of cells showing no event, potentially indicative of a cell cycle delay within the limits of the tracking period. Greater than 250 progenitor cells were tracked through one to three events to assess proliferation dynamics. Table 1 shows typical results in which both cell lines show ~96% of their mitotic events as normal (bipolar). MT-1 overexpression did not influence the frequency of the low-level abnormal events, including polyploidy, multipolar divisions and cell death. Figure 2*A* graphically shows the time-resolved event data for the duration of mitosis and the mean intermitotic times for progenitor cells and subsequent progeny. The data show no significant impact of MT-1 expression on intermitotic or mitotic duration.

Subclones of the CHO-K1 MT-1 transfectant 2.20.1 were generated to provide a panel to explore the potential for clonal variation, and MT-1 expressing subclones were found to show no abnormalities in steady-state cell cycle distribution, as determined by flow cytometry, compared with the CHO-K1 parent line (Fig. 2*B*).

Subclone analysis of MT-1 transfectants. CHO-K1 MT-1 transfectant 2.20.1 subclones were analyzed for relative levels of MT-1 expression by flow cytometry (Fig. 3*A*) and cellular protein location by laser scanning confocal microscopy (examples shown in Fig. 3*B*). The flow cytometric analysis corresponded to the MT-1 immunoblotting results for the ranking of the reference lines CHO-K1 parent and transfectant clones 1.5.1 and 2.20.1. Figure 3*A* shows the subclones ranked for range of MT-1 expression. Laser scanning confocal microscopy permitted a closer study of MT-1 distribution and was

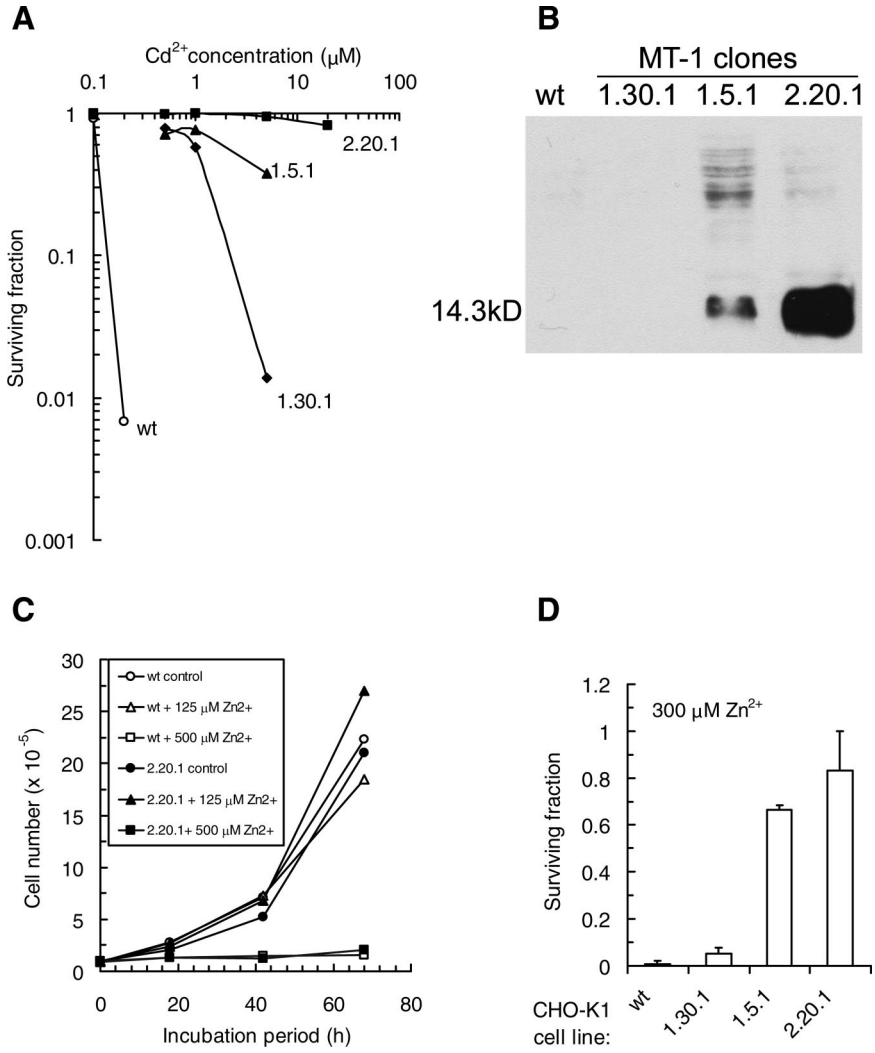

Fig. 1. *A*: cadmium sensitivity of Chinese hamster ovary (CHO)-K1 wild-type (WT) and metallothionein (MT)-1 transfectants determined by clonogenic survival. Data are mean values derived from triplicate determinations. *B*: immunoblot for MT-1 protein expression using a mouse monoclonal antibody E9 to isoforms I and II. *C*: CHO-K1 MT-1 2.20.1 transfectant and WT both show rapid and complete growth inhibition at 500 μM Zn^{2+}. *D*: CHO-K1 MT-1 transfectants show enhanced resistance to Zn^{2+} toxicity. Data are mean values (± SD) derived from 3 experiments.

carried out on all subclones (Fig. 3*B*). An example image for CHO-K1 (Fig. 3*Ba*) has been set to show the near-background levels of MT detected by immunofluorescence, while an optical slice of the MT-1 transfectant 2.20.1 (Fig. 3*Bb*) and a projection of an image stack (Fig. 3*Bc*) show the nonnuclear location and enhanced whole cell expression, respectively. Colcemid was used to capture subclone 32D5 cells in mitosis, providing a highly synchronized population with no nuclear membranes (Fig. 3*Bd*), revealing homogenous distribution through the population and within individual cells but no evidence of any chromosomal association. Similar exemplar results were obtained for asynchronous subclone 64C1 cells (Fig. 3*Be*: optical section; Fig. 3*Bf*: projection).

Subclone analysis of MT-1 transfectants: intracellular free zinc. CHO-K1 MT-1 transfectant 2.20.1 subclones were analyzed by flow cytometry and ranked (Fig. 4*A*) for relative levels of free intracellular Zn^{2+}, defined as that fraction available to the Zinquin fluorescent probe (41, 44). The transfectant 2.20.1 showed a slightly elevated (1.7-fold) increase in free-Zn^{2+} compared with the low levels in the CHO-K1 parent. The

Table 1. *Frequency of morphologically distinct events during time-lapse tracking of proliferating cells*

	%Event Type					
Event	Mitosis	Polyploidy	Multipolar Division	Death	Unknown*	No Event
CHO-K1						
1st	98.9	0.7	0.0	0.4	0.0	0.0
2nd	95.6	0.9	0.2	0.7	1.8	0.7
3rd	92.6	0.2	0.0	0.0	5.7	1.5
MT-1 transfectant clone 2.20.1						
1st	98.1	1.2	0.0	0.4	0.4	0.0
2nd	97.1	0.8	0.0	0.2	1.4	0.6
3rd	93.4	0.2	0.0	0.7	4.6	1.1

CHO, Chinese hamster ovary; MT-1, metallothionein-1. *Unknown indicates the loss of a tracked cell from the field of view.

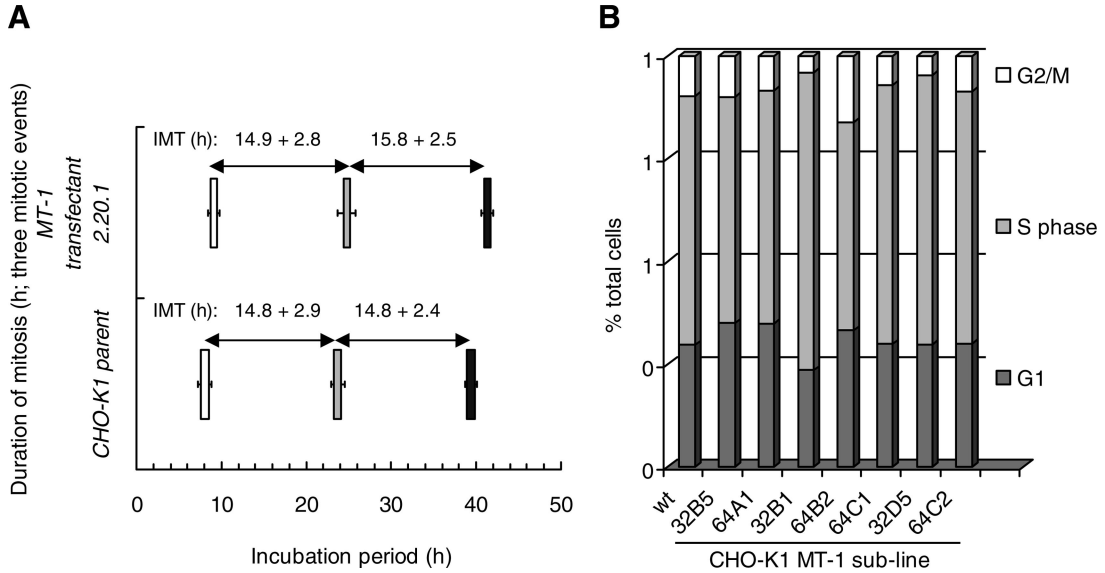

Fig. 2. *A*: CHO-K1 cells and MT-1 transfectant 2.20.1 show similar durations for mitosis (value shown as width of bar; ±SD) and mean intermitotic times (IMT; ±SD) derived for individual cells tracked to first mitotic event (open bars), second mitotic event for a daughter cell (shaded bars), and third mitotic event for a granddaughter cell (solid bars). *B*: sublines of CHO-K1 MT-1 transfectant 2.20.1 show no abnormalities in cell cycle distributions as determined by flow cytometry. Data are derived from a single representative experiment ($n = 2$).

2.20.1 subclones, with homogenous MT-1 expression, showed free-Zn^{2+} levels up to 12-fold greater than the CHO-K1 parent. Figure 4*B* shows the application of multiphoton imaging to Zinquin-Zn^{2+} loaded subclone 64C2 cells (*left* panel transmission and *right* panel fluorescence) in which Zinquin-Zn^{2+} associated fluorescence is cytoplasmic and punctuate. The transmission image indicates recently divided cells (arrowed) displaying Zinquin-Zn^{2+} levels similar to other cells in the field, suggesting a lack of correlation with cell cycle age.

Subclone analysis of MT-1 transfectants: Zn^{2+} toxicity and MT-1 expression. To explore the impact of MT-1 expression on free Zn^{2+} and Zn^{2+} toxicity, correlated data sets were plotted for the subclone panel (Fig. 5). The trend line for MT-1 vs. free Zn^{2+} (logarithmic; $R^2 = 0.82$) shows a positive relationship, although low-level enhancement of MT-1 expression does not significantly contribute to an increase in free Zn^{2+} (Fig. 5*A*). Furthermore, a 10-fold enhancement in MT-1 levels corresponds to a ~2-fold increase in free Zn^{2+}, a correlation similar to that observed for induced levels of MTs in human cells exposed to 50 μM exogenous Zn^{2+} (27). Correlating MT-1 expression with the logarithm of surviving fraction, at the reference concentration of 300 μM Zn^{2+}, yields a positive relationship (logarithmic; $R^2 = 0.74$; Fig. 5*B*). To gain an overview of the extent of such MT-1-related resistance,

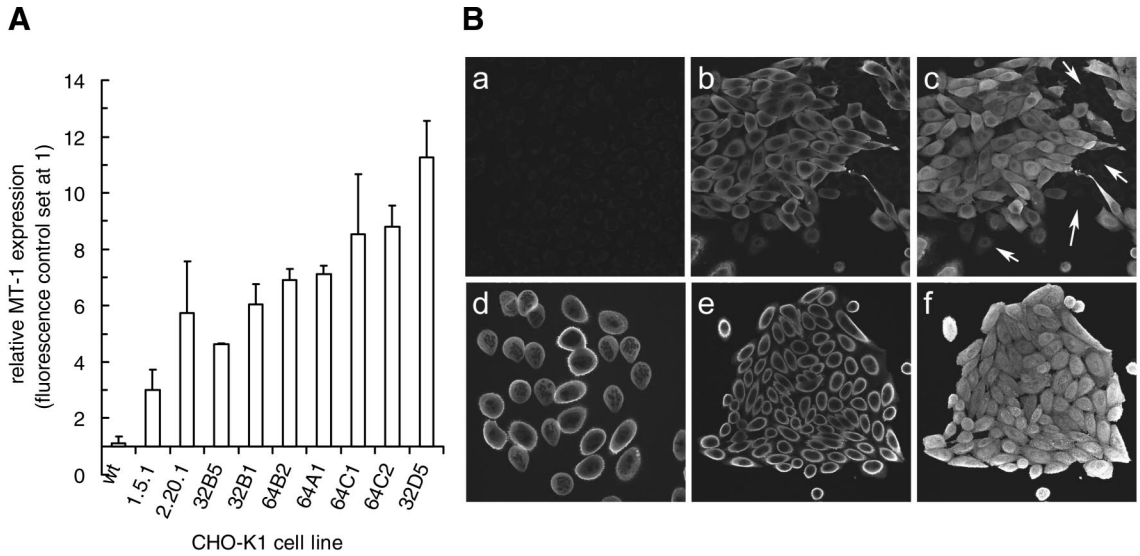

Fig. 3. MT-1 expression and subcellular distribution in cell lines. *A*: MT-1 transfectants 1.5.1 and 2.20.1 and the subclones of 2.20.1 show a range of significantly elevated MT-1 levels as determined by flow cytometry. Data are ranked mean values (±SD) derived from 3 experiments. *B*: laser scanning confocal microscopy of MT-1 distribution in CHO-K1 (*a*), MT-1 transfectant 2.20.1 (*b*: optical section; *c*: projection), subclone 32D5 of 2.20.1 (*d*: optical of mitotic cells captured using colcemid treatment), and subclone 64C1 (*e*: optical section; *f*: projection). Images reveal the very low level of expression in WT CHO-K1 cells (*a*), heterogeneous expression in 2.20.1 (*b* and *c*; arrows indicate the presence of low expression cells), but homogeneous expression in subclones, irrespective of cell cycle stage (*d–f*). Panels are either maximal pixel projections of image stacks, or single optical sections (512 × 512 μm).

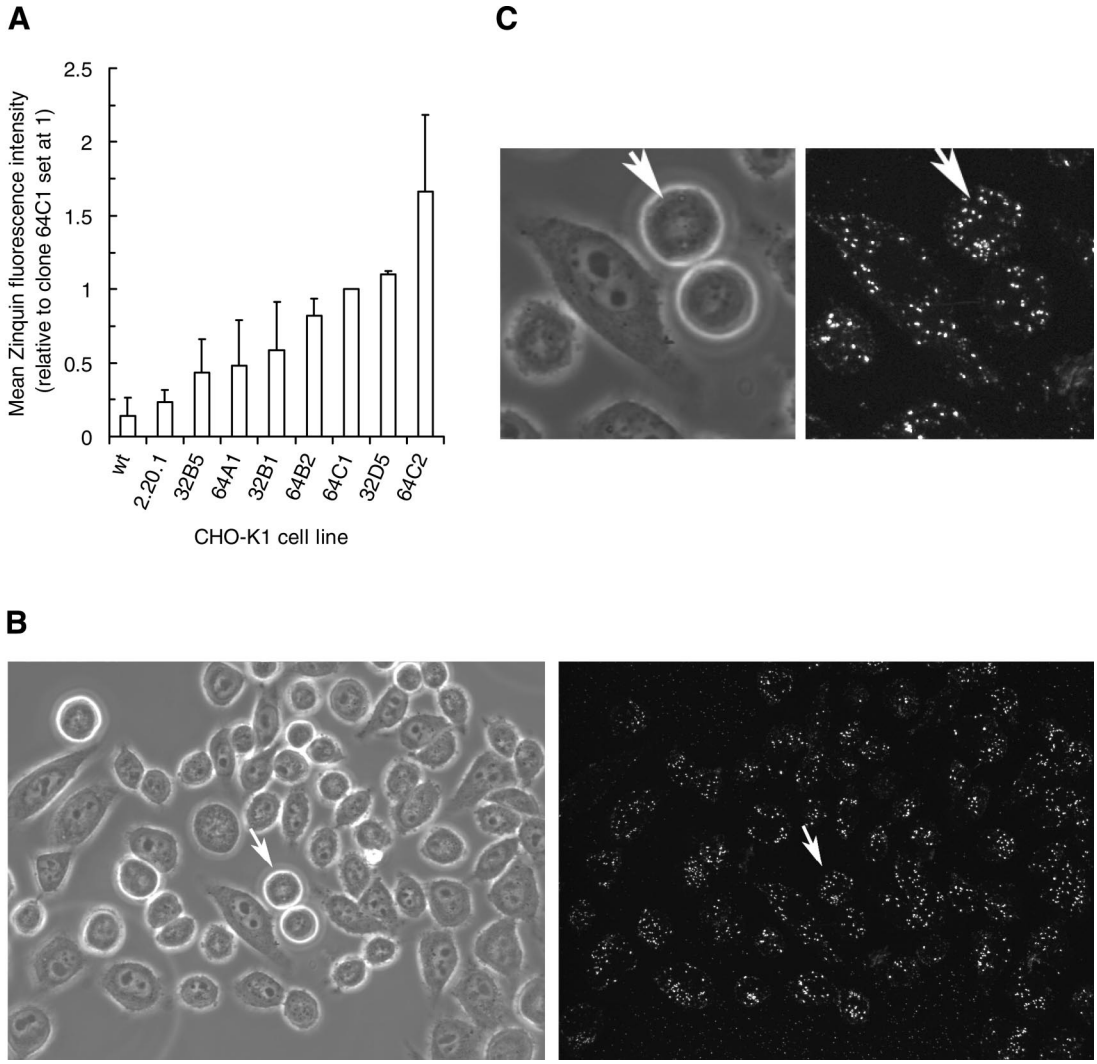

Fig. 4. *A*: flow cytometric analysis of relative fluorescence of Zinquin in WT, MT-1 transfectant 2.20.1, and its subclones revealing the ranking of differential expression patterns. Data are ranked mean values (±SD) derived from 3 experiments. *B*: laser scanning confocal microscopy of Zinquin distribution in CHO-K1 MT-1 transfectant 2.20.1 subclone 64C2 showing typical punctuate cytoplasmic locations. Transmission (*left*) and fluorescence (*right*) images are 512 × 512 μm. *C*: detail of cell marked by arrows in *B*: transmission (*left*) and fluorescence (*right*).

IC values for the ability of exogenous Zn^{2+} to reduce subclone survival by 20, 50, and 90% (i.e., IC_{20}, IC_{50}, and IC_{90}, respectively) were calculated from clonogenic cell survival data, yielding exponential fitted trend lines with R^2 values of 0.84, 0.63, and 0.85, respectively (Fig. 5*C*). The trends show that, over the toxicity range of 20–90% inhibition, resistance is more efficiently enhanced by the lower (<4-fold) levels of MT-1 overexpression than the higher levels (10-fold), suggesting that MT-1 has a limited effective range and saturable capacity for effecting resistance to Zn^{2+} toxicity.

DISCUSSION AND CONCLUSIONS

The present study reveals a clear relationship in our CHO-K1 cell system between MT-1 expression and protection from zinc toxicity, although such protection is restricted and easily overwhelmed. There is no evidence that MT-1 overexpression, at levels capable of protecting significantly against cadmium and zinc toxicity, impacts on normal progression of the cell cycle, suggesting that, under ambient conditions, the availability of Zn^{2+} is not limiting. Previous reports of an increase in MT in proliferating cells, with the levels returning to what they initially were on growth arrest (33, 45), were at least supportive of an association of MTs with cell proliferation. A previous study has shown impaired hepatic regeneration in MT-I/II knockout mice after partial hepatectomy (35), while liver cells of MT-null mice with no functional MT are unable to regenerate after hepatic oxidative stress-induced injury following thioacetamide exposure (34). Thus it is possible that a limitation on proliferation can be related to MT expression under conditions in which cells need to reenter the cell cycle from a quiescent state under growth factor control. Our study suggests that MT levels may be less relevant once cells have entered a continuously proliferating state. Our working hypothesis was that, under normal conditions, cells with different MT levels could experience varying degrees of constraint on cell cycle control through two routes.

The first route is constraint through changes in the availability of free zinc for the operation of regulatory pathways,

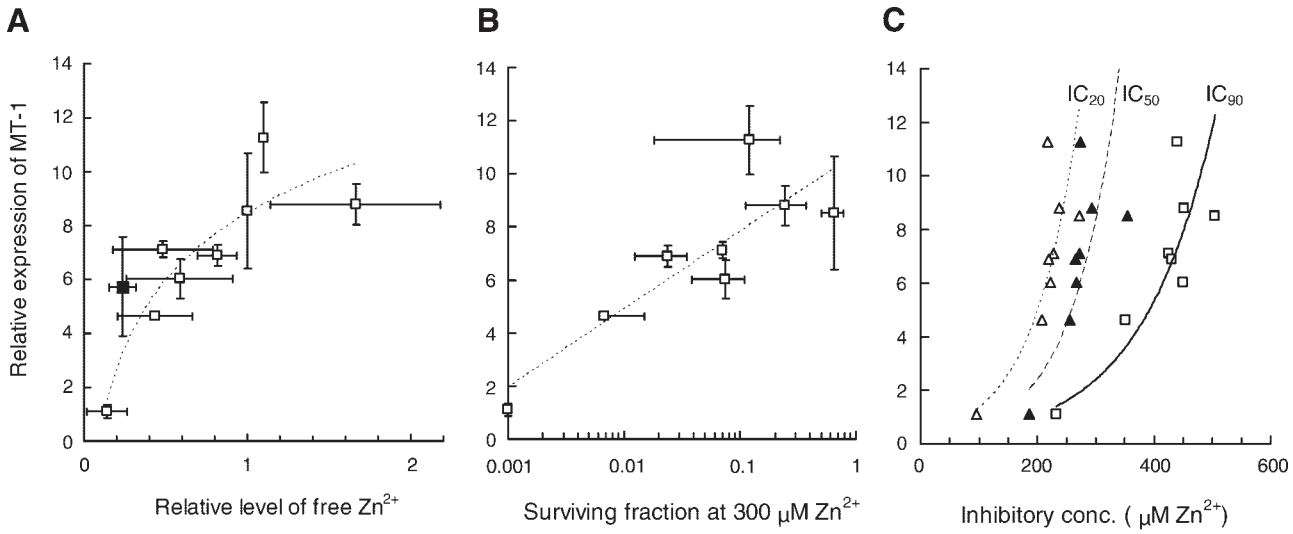

Fig. 5. *A*: relationship between MT-1 expression and the relative level of free Zn^{2+} determined by flow cytometry. Relative MT-1 expression is given by the fold increase above nonspecific antibody binding control. Free Zn^{2+} is given by relative level of Zinquin-specific fluorescence, using clone 64C1 as the biological control set at a value of 1 for background-corrected mean fluorescence intensity of 10^4 cells. Data are mean values (±SD) derived from 3–4 experiments. Trend line shows relationship for WT and subclone data alone; 2.20.1 (solid square) included for reference. *B*: relationship between MT-1 expression and the resistance of clonogenic potential to continuous presence of Zn^{2+} toxicity for collected WT and subclones. Data are mean values (±SD) derived from 3–4 experiments. *C*: relationship between MT-1 expression and the resistance to Zn^{2+} toxicity for collected WT and subclones. Figure shows relationships at inhibition concentrations (IC) of 20% (△), 50% (▲), and 90% (□), representing cell survival levels of 80, 50, and 10%, respectively. Data are mean values (±SD) derived from 3–4 experiments.

including those associated with basal stress responses. Our laboratory has previously described the use of flow cytometry to track changes in intracellular Zn^{2+} using the fluorescent probe Zinquin (61, 62) and to determine the characteristic formation of Zinquin-Zn^{2+} complexes in cytoplasmic vesicles using two-photon excitation microscopy (41, 44). In the present study, these approaches were used to determine relative levels of free intracellular Zn^{2+} and to confirm the enhanced cytoplasmic location of Zinquin-Zn^{2+} complexes in MT-1 overexpressing cells. We conclude that neither the degree of enforced overexpression of MT-1 nor associated enhanced basal levels of free Zn^{2+} impact on the normal progression or the steady-state distribution of cells in the cell cycle.

The present study shows that the degree of enforced overexpression of MT-1 showed a positive relationship with the basal levels of free-intracellular resting levels of Zn^{2+} within the subclone panel. In a study by Coyle et al. (11), Zinquin was incubated liver cytosolic fractions, and the sensor was found to fluoresce with free zinc, protein-bound zinc, and MT-incorporated zinc. Furthermore, there was evidence of a promotion of MT degradation and a reduced fluorescence of the sensor with un-degraded zinc-MT (~20% of the expected intensity) (11). Thus using Zinquin as a zinc sensor in cells with varying levels of MT, as in the present study, may be problematic. However, we have tested the stability of 14.3-kDa MT in the high-expressing subclone exposed to Zinquin and found no evidence of significant in situ degradation (data not shown). We suggest that zinc mobilization via Zinquin-induced MT turnover in CHO-K1 is minimal. Background-corrected total cellular fluorescence of Zinquin can be considered a compound of signal intensity of sensor binding with free zinc, protein-bound zinc, and a restricted reporting of MT-incorporated zinc.

The use of Zinquin did not appear to drive any degradation of MT-1 (data not shown) in reporting the enhanced levels of free Zn^{2+}, and it is likely that the enhanced Zn^{2+} basal levels in MT-1 overexpressing cells represent a partial Zinquin chelation of zinc at the MT-1 beta domain. A previous study using a different zinc sensor, ZP1 (27), indicated that human cells grown in high-zinc environments can elevate their levels of MTs, giving rise to a ~11-fold increase in total cellular zinc levels but only a moderate (2.4-fold) elevation in free zinc accessible to the fluorescent ZP1 reporter. In keeping with this finding, the present study shows that intracellular zinc ion availability is strictly regulated by these proteins.

The second route is constraint through the protective effects of MTs on cell cycle-retarding basal levels of oxidative stress. Such stress could generate proliferation-retarding signals, given that normal cellular respiration generates potentially damaging reactive oxygen species. Although overexpression of MT-1 has been reported to significantly protect mitochondria from both NO donor and Zn^{2+}-mediated disruption and the subsequent induction of cell death, it did not appear to alter basal oxidative stress, as measured by the levels of reactive oxygen species (54). The potential for basal levels of endogenous (e.g., oxidative) stress, associated with abnormal zinc availability (14), to exert any cell cycle disturbing effects will depend not only on the availability of protective mechanisms for a given type of stress, but also on the ability of the cellular system to enact a cell cycle-linked response. In general, it appears that cytoplasmic MT protects against cytotoxicity, whereas nuclear MT protects against genotoxicity (1, 2, 8, 40, 57, 58). Our distribution study indicated a primarily cytoplasmic location for enforced MT-1 overexpression. Thus there is no evidence of low level of cytoplasmic stress signaling, relevant for MT-1 modulation, operating to restrict growth potential in the CHO-K1 system. Any low-level genotoxic stress, for example, of the form capable of transduction through a p53 signaling pathways for cell cycle arrest and cell death, is

unlikely to be assessable by the MT-1 overexpression panel. A recent study suggests that, under mild deficiencies in zinc supply, the inhibition of cell cycle progression is independent of the p53 downstream cyclin-dependent kinase inhibitor p21 (56), whereas a small interfering RNA study indicates that high zinc status can lead to an upregulation of p53 expression and a p21 enforced G2/M blockage (55). However, our findings suggest that cells with overexpression of MT-1 are not operating under conditions of reduced availability of free zinc but would be expected to be resistant to high-zinc status-induced arrest.

Considering the converse effect of the loss of MT expression on divalent metal sensitivity, a previous study by Kondo et al. (22) used primary cultured mouse embryonic cells from mice with disrupted MT-I and -II genes. MT−/− and MT+/+ cell strains were established by transformation using SV40 large T antigen. The resulting cell lines were found to have similar cell cycle characteristics (22). The transformed rodent cell system, used in the present study, may be somewhat desensitized to genomic stress induction, given an ambiguous role for the tumor suppressor p53 in CHO cell cycle arrest and apoptosis (7, 15, 46, 47). CHO-K1 cells demonstrate dose-dependent, p53-independent G2/M arrest, but a failure to regulate UV-induced apoptosis (7). CHO-K1 cells have mutant p53 sequence (a mutation in codon 211), and the noninduction of p21(Waf1/Cip1) protein (7) appears to account for a lack of G1 checkpoint function observed for both X irradiation (15) and UV irradiation (46). However, CHO cells are competent for cell cycle arrest in response to cadmium (59), and they appear to be more sensitive than human cell lines (59), with a previous study on CHO-K1 cells reporting G2/M phase arrest between 12 and 36 h after exposure to 4 μM cadmium (60). Taken together, the findings suggest that the loss or gain of MT expression does not impact on any growth-retarding effects of basal levels of oxidative stress in these late cell cycle checkpoint-compromised cells. The situation may be different in cells capable of enacting checkpoint engagement. Here the metal-depleted species apo-MT does have the potential to remove zinc from p53, an important regulator of genomic stress-related cell cycle arrest, and inactivate it in a similar manner to other zinc chelators (17). Thus, if persistent overexpression of apo-MT exists in tumor cells, driven by MT overexpression and insufficient Zn^{2+} supply, it may act to remove restraints on survival and proliferation through induction of a quasi-p53 null state (17, 30).

In physiological terms, healthy human subjects show plasma zinc levels of ~12 μM (38). In toxicological situations, elevated levels can be toxic to cells, a previous study indicating that, in neuroblastoma (N2α) cell cultures exposed to 100 μM of zinc (4–24 h), loss of viability was attributable to a generation of reactive oxygen species and an activation of the MAP kinase pathway (12). Under conditions of imposed zinc stress (e.g., 300 μM Zn^{2+}), CHO-K1 cells clearly show the capacity for cycle arrest. Under these more severe stress conditions, expression of MT-1 has a clear effect on the ability of cells to resist the antiproliferative effects of Zn^{2+} oversupply up to a limiting threshold of ~500 μM Zn^{2+}. Beattie et al. (4) showed that concentrations of soluble MT can increase upon exposure of an MT overexpressing (MToex) CHO-K1 cell line to Zn^{2+}, whereas the levels of soluble MT in the wild-type parent line remained unchanged. The concentration-related increase in MT levels in the MT-1 transfectant CHO-K1 cells (termed MToex), as used in the present study, could not be attributed to the induction of MT expression, because the promoter used for the MT gene construct is noninducible by metals. Beattie et al. (4) suggested that this effect may be due to a stabilization of the MT protein or mRNA directly or indirectly by zinc. The further study of zinc-binding MT levels would provide clarification of the physiological consequences of MT overexpression under toxic and subtoxic metal ion concentrations, as defined in the present study.

We have noted that high-level zinc exposure is now being considered for therapeutic applications, where stress induction or indeed cell death is actively sought. For example, cellular level manipulation of zinc accumulation to toxic levels, via analogs of zinc ionophore 1-hydroxypyridine-2-thione, is currently being considered as a novel approach in cancer therapeutics (25). Furthermore, exogenously supplied zinc may extend the application of the antitumor agent tumor necrosis factor (TNF) by inducing a protective effect against the generation of TNF-induced inflammation in at-risk organs (49). The principle is to use zinc to induce the heat shock protein 70 in such organs, including the gastrointestinal tract, thereby preventing a potentially lethal systemic inflammatory response by reducing cytokine liberation (49). Protection against TNF-induced lethality by zinc appears to be independent of MT (51), suggesting that any modulation by MT of zinc ion availability at the cellular level is limited. The present study underlines this limited buffering capacity.

It is apparent that the protective effect of MT-1 is limited (2-fold modification for the inhibitory Zn^{2+} concentration) compared with the massive degree of protection (>100-fold) afforded for cadmium toxicity. Kondo et al. (22), in the study on MT−/− and MT+/+ cell strains, reported no increase in the sensitivity to Zn, Cu, Hg, or Ni occurred in MT−/− cells with IC_{50} values of ~148–158 μM Zn^{2+} for a 48-h exposure, as determined by a tetrazolium dye assay for residual metabolic potential. We conclude that the normal levels of MT expression in rodent cells are readily overwhelmed in terms of their capacity to protect against the toxicity of Zn^{2+} oversupply. We suggest that our resolution of the zinc resistance relationship with MT-1 reported here was made possible by the use of subcloned lines, verified for their level and homogeneity of MT-1 protein expression and the use of the wider dynamic range of a clonogenic analysis for cell survival. The present study supports the view that, under normal conditions, MTs are not necessary (36) for proliferation, but they could serve as a limited repository of metal, reducing toxicity, when cells are exposed to zinc oversupply.

ACKNOWLEDGMENTS

We are grateful for the laboratory support by J. Pocock, S. Davies, and S. Chappell (Cardiff) and the contribution of Dr. Hassan Zaidi (Aberdeen) in generating the CHO-K1 transfectant cell lines.

GRANTS

The work was supported by research grants to P. J. Smith and R. J. Errington from the UK Research Councils' Basic Technology Research Programme, the Biotechnology and Biological Sciences Research Council, and the Association for International Cancer Research. E. Furon is an Engineering and Physical Sciences Research Council CASE Student.

REFERENCES

1. **Apostolova MD, Cherian MG.** Delay of M-phase onset by aphidicolin can retain the nuclear localization of zinc and metallothionein in 3T3–L1 fibroblasts. *J Cell Physiol* 183: 247–253, 2000.
2. **Apostolova MD, Ivanova IA, Cherian MG.** Signal transduction pathways, and nuclear translocation of zinc and metallothionein during differentiation of myoblasts. *Biochem Cell Biol* 78: 27–37, 2000.
3. **Aschner M, Rising L, Mullaney KJ.** Differential sensitivity of neonatal rat astrocyte cultures to mercuric chloride (MC) and methylmercury (MeHg): studies on K^+ and amino acid transport and metallothionein (MT) induction. *Neurotoxicology* 17: 107–116, 1996.
4. **Beattie JH, Owen HL, Wallace SM, Arthur JR, Kwun IS, Hawksworth GM, Wallace HM.** Metallothionein overexpression and resistance to toxic stress. *Toxicol Lett* 157: 69–78, 2005.
5. **Beyersmann D, Hechtenberg S.** Cadmium, gene regulation, and cellular signalling in mammalian cells. *Toxicol Appl Pharmacol* 144: 247–261, 1997.
6. **Cai L, Li XK, Song Y, Cherian MG.** Essentiality, toxicology and chelation therapy of zinc and copper. *Curr Med Chem* 12: 2753–2763, 2005.
7. **Chang YC, Liao CB, Hsieh PY, Liou ML, Liu YC.** Expression of tumor suppressor p53 facilitates DNA repair but not UV-induced G2/M arrest or apoptosis in Chinese hamster ovary CHO-K1 cells. *J Cell Biochem* 103: 528–537, 2008.
8. **Cherian MG, Apostolova MD.** Nuclear localization of metallothionein during cell proliferation and differentiation. *Cell Mol Biol (Noisy-le-grand)* 46: 347–356, 2000.
9. **Colvin RA, Bush A, Volitakis I, Fontaine CP, Thomas D, Kikuchi K, Holmes WR.** Insights into Zn^{2+} homeostasis in neurons from experimental and modeling studies. *Am J Physiol Cell Physiol* 294: C726–C742, 2008.
10. **Coyle P, Philcox JC, Carey LC, Rofe AM.** Metallothionein: the multipurpose protein. *Cell Mol Life Sci* 59: 627–647, 2002.
11. **Coyle P, Zalewski PD, Philcox JC, Forbes IJ, Ward AD, Lincoln SF, Mahadevan I, Rofe AM.** Measurement of zinc in hepatocytes by using a fluorescent probe, zinquin: relationship to metallothionein and intracellular zinc. *Biochem J* 303: 781–786, 1994.
12. **Daniels WM, Hendricks J, Salie R, van Rensburg SJ.** A mechanism for zinc toxicity in neuroblastoma cells. *Metab Brain Dis* 19: 79–88, 2004.
13. **Garrett SH, Somji S, Todd JH, Sens MA, Sens DA.** Differential expression of human metallothionein isoform I mRNA in human proximal tubule cells exposed to metals. *Environ Health Perspect* 106: 825–832, 1998.
14. **Ho E, Courtemanche C, Ames BN.** Zinc deficiency induces oxidative DNA damage and increases p53 expression in human lung fibroblasts. *J Nutr* 133: 2543–2548, 2003.
15. **Hu T, Miller CM, Ridder GM, Aardema MJ.** Characterization of p53 in Chinese hamster cell lines CHO-K1, CHO-WBL, and CHL: implications for genotoxicity testing. *Mutat Res* 426: 51–62, 1999.
16. **Jasani B, Campbell F, Navabi H, Schmid KW, Williams GT.** Clonal overexpression of metallothionein is induced by somatic mutation in morphologically normal colonic mucosa. *J Pathol* 184: 144–147, 1998.
17. **Jasani B, Schmid KW.** Significance of metallothionein overexpression in human tumours. *Histopathology* 31: 211–214, 1997.
18. **Jin T, Lu J, Nordberg M.** Toxicokinetics and biochemistry of cadmium with special emphasis on the role of metallothionein. *Neurotoxicology* 19: 529–535, 1998.
19. **Kao FT, Puck TT.** Genetics of somatic mammalian cells. VII. Induction and isolation of nutritional mutants in Chinese hamster cells. *Proc Natl Acad Sci USA* 60: 1275–1281, 1968.
20. **Klaassen CD, Liu J.** Metallothionein transgenic and knock-out mouse models in the study of cadmium toxicity. *J Toxicol Sci* 23, *Suppl* 2: 97–102, 1998.
21. **Koizumi S, Suzuki K, Ogra Y, Yamada H, Otsuka F.** Transcriptional activity and regulatory protein binding of metal-responsive elements of the human metallothionein-IIA gene. *Eur J Biochem* 259: 635–642, 1999.
22. **Kondo Y, Yanagiya T, Himeno S, Yamabe Y, Schwartz D, Akimoto M, Lazo JS, Imura N.** Simian virus 40-transformed metallothionein null cells showed increased sensitivity to cadmium but not to zinc, copper, mercury or nickel. *Life Sci* 64: PL145–PL150, 1999.
23. **Liang L, Fu K, Lee DK, Sobieski RJ, Dalton T, Andrews GK.** Activation of the complete mouse metallothionein gene locus in the maternal deciduum. *Mol Reprod Dev* 43: 25–37, 1996.
24. **Lin KA, Chen JH, Lee DF, Lin LY.** Alkaline induces metallothionein gene expression and potentiates cell proliferation in Chinese hamster ovary cells. *J Cell Physiol* 205: 428–436, 2005.
25. **Magda D, Lecane P, Wang Z, Hu W, Thiemann P, Ma X, Dranchak PK, Wang X, Lynch V, Wei W, Csokai V, Hacia JG, Sessler JL.** Synthesis and anticancer properties of water-soluble zinc ionophores. *Cancer Res* 68: 5318–5325, 2008.
26. **Maier H, Jones C, Jasani B, Ofner D, Zelger B, Schmid KW, Budka H.** Metallothionein overexpression in human brain tumours. *Acta Neuropathol (Berl)* 94: 599–604, 1997.
27. **Malavolta M, Costarelli L, Giacconi R, Muti E, Bernardini G, Tesei S, Cipriano C, Mocchegiani E.** Single and three-color flow cytometry assay for intracellular zinc ion availability in human lymphocytes with Zinpyr-1 and double immunofluorescence: relationship with metallothioneins. *Cytometry A* 69: 1043–1053, 2006.
28. **Marquez N, Chappell SC, Sansom OJ, Clarke AR, Court J, Errington RJ, Smith PJ.** Single cell tracking reveals that Msh2 is a key component of an early-acting DNA damage-activated G2 checkpoint. *Oncogene* 22: 7642–7648, 2003.
29. **Marquez N, Chappell SC, Sansom OJ, Clarke AR, Teesdale-Spittle P, Errington RJ, Smith PJ.** Microtubule stress modifies intra-nuclear location of Msh2 in mouse embryonic fibroblasts. *Cell Cycle* 3: 662–671, 2004.
30. **McCluggage WG, Maxwell P, Hamilton PW, Jasani B.** High metallothionein expression is associated with features predictive of aggressive behaviour in endometrial carcinoma. *Histopathology* 34: 51–55, 1999.
31. **Meneghini R.** Iron homeostasis, oxidative stress, and DNA damage. *Free Radic Biol Med* 23: 783–792, 1997.
32. **Miles AT, Hawksworth GM, Beattie JH, Rodilla V.** Induction, regulation, degradation, and biological significance of mammalian metallothioneins. *Crit Rev Biochem Mol Biol* 35: 35–70, 2000.
33. **Nagel WW, Vallee BL.** Cell cycle regulation of metallothionein in human colonic cancer cells. *Proc Natl Acad Sci USA* 92: 579–583, 1995.
34. **Oliver JR, Jiang S, Cherian MG.** Augmented hepatic injury followed by impaired regeneration in metallothionein-I/II knockout mice after treatment with thioacetamide. *Toxicol Appl Pharmacol* 210: 190–199, 2006.
35. **Oliver JR, Mara TW, Cherian MG.** Impaired hepatic regeneration in metallothionein-I/II knockout mice after partial hepatectomy. *Exp Biol Med (Maywood)* 230: 61–67, 2005.
36. **Palmiter RD.** The elusive function of metallothioneins. *Proc Natl Acad Sci USA* 95: 8428–8430, 1998.
37. **Palmiter RD, Findley SD.** Cloning and functional characterization of a mammalian zinc transporter that confers resistance to zinc. *EMBO J* 14: 639–649, 1995.
38. **Potocnik FC, van Rensburg SJ, Hon D, Emsley RA, Moodie IM, Erasmus RT.** Oral zinc augmentation with vitamins A and D increases plasma zinc concentration: implications for burden of disease. *Metab Brain Dis* 21: 139–147, 2006.
39. **Reyes JG.** Zinc transport in mammalian cells. *Am J Physiol Cell Physiol* 270: C401–C410, 1996.
40. **Schwarz MA, Lazo JS, Yalowich JC, Reynolds I, Kagan VE, Tyurin V, Kim YM, Watkins SC, Pitt BR.** Cytoplasmic metallothionein overexpression protects NIH 3T3 cells from tert-butyl hydroperoxide toxicity. *J Biol Chem* 269: 15238–15243, 1994.
41. **Smith PJ, Blunt N, Wiltshire M, Hoy T, Teesdale-Spittle P, Craven MR, Watson JV, Amos WB, Errington RJ, Patterson LH.** Characteristics of a novel deep red/infrared fluorescent cell-permeant DNA probe, DRAQ5, in intact human cells analyzed by flow cytometry, confocal and multiphoton microscopy. *Cytometry* 40: 280–291, 2000.
42. **Smith PJ, Marquez N, Wiltshire M, Chappell S, Njoh K, Campbell L, Khan IA, Silvestre O, Errington RJ.** Mitotic bypass via an occult cell cycle phase following DNA topoisomerase II inhibition in p53 functional human tumor cells. *Cell Cycle* 6: 2071–2081, 2007.
43. **Smith PJ, Wiltshire M, Chin SF, Rabbitts P, Soues S.** Cell cycle checkpoint evasion and protracted cell cycle arrest in X-irradiated small-cell lung carcinoma cells. *Int J Radiat Biol* 75: 1137–1147, 1999.
44. **Smith PJ, Wiltshire M, Davies S, Chin SF, Campbell AK, Errington RJ.** DNA damage-induced [Zn(2+)](i) transients: correlation with cell cycle arrest and apoptosis in lymphoma cells. *Am J Physiol Cell Physiol* 283: C609–C622, 2002.
45. **Studer R, Vogt CP, Cavigelli M, Hunziker PE, Kagi JH.** Metallothionein accretion in human hepatic cells is linked to cellular proliferation. *Biochem J* 328: 63–67, 1997.

46. **Tzang BS, Lai YC, Hsu M, Chang HW, Chang CC, Huang PC, Liu YC.** Function and sequence analyses of tumor suppressor gene p53 of CHO.K1 cells. *DNA Cell Biol* 18: 315–321, 1999.
47. **Tzang BS, Lai YC, Liu YC.** UV-induced but P53 independent apoptotic death in CHO. K1 cells is promoted by M phase inhibitors. *In Vitro Cell Dev Biol Anim* 35: 17–18, 1999.
48. **Vallee BL.** Introduction to metallothionein. *Methods Enzymol* 205: 3–7, 1991.
49. **Van Molle W, Van Roy M, Van Bogaert T, Dejager L, Van Lint P, Vanlaere I, Sekikawa K, Kollias G, Libert C.** Protection of zinc against tumor necrosis factor induced lethal inflammation depends on heat shock protein 70 and allows safe antitumor therapy. *Cancer Res* 67: 7301–7307, 2007.
50. **Vasak M.** Advances in metallothionein structure and functions. *J Trace Elem Med Biol* 19: 13–17, 2005.
51. **Waelput W, Broekaert D, Vandekerckhove J, Brouckaert P, Tavernier J, Libert C.** A mediator role for metallothionein in tumor necrosis factor-induced lethal shock. *J Exp Med* 194: 1617–1624, 2001.
52. **Wallace SM, Zaidi H, Arthur JR, Bremner I.** Effect of zinc on metallothionein content of CHO cells transfected with metallothionein gene under the control of a non-inducible promoter. *Biochem Soc Trans* 24: 237S, 1996.
53. **Wellinghausen N, Fischer A, Kirchner H, Rink L.** Interaction of zinc ions with human peripheral blood mononuclear cells. *Cell Immunol* 171: 255–261, 1996.
54. **Wiseman DA, Wells SM, Wilham J, Hubbard M, Welker JE, Black SM.** Endothelial response to stress from exogenous Zn^{2+} resembles that of NO-mediated nitrosative stress and is protected by MT-1 overexpression. *Am J Physiol Cell Physiol* 291: C555–C568, 2006.
55. **Wong SH, Shih RS, Schoene NW, Lei KY.** Zinc-induced G2/M blockage is p53 and p21 dependent in normal human bronchial epithelial cells. *Am J Physiol Cell Physiol* 294: C1342–C1349, 2008.
56. **Wong SH, Zhao Y, Schoene NW, Han CT, Shih RS, Lei KY.** Zinc deficiency depresses p21 gene expression: inhibition of cell cycle progression is independent of the decrease in p21 protein level in HepG2 cells. *Am J Physiol Cell Physiol* 292: C2175–C2184, 2007.
57. **Woo ES, Lazo JS.** Nucleocytoplasmic functionality of metallothionein. *Cancer Res* 57: 4236–4241, 1997.
58. **Woo ES, Monks A, Watkins SC, Wang AS, Lazo JS.** Diversity of metallothionein content and subcellular localization in the National Cancer Institute tumor panel. *Cancer Chemother Pharmacol* 41: 61–68, 1997.
59. **Xie J, Shaikh ZA.** Cadmium induces cell cycle arrest in rat kidney epithelial cells in G2/M phase. *Toxicology* 224: 56–65, 2006.
60. **Yang PM, Chiu SJ, Lin KA, Lin LY.** Effect of cadmium on cell cycle progression in Chinese hamster ovary cells. *Chem Biol Interact* 149: 125–136, 2004.
61. **Zalewski PD, Forbes IJ, Betts WH.** Correlation of apoptosis with change in intracellular labile Zn(II) using zinquin [(2-methyl-8-p-toluenesulphonamido-6-quinolyloxy)acetic acid], a new specific fluorescent probe for Zn(II). *Biochem J* 296: 403–408, 1993.
62. **Zalewski PD, Millard SH, Forbes IJ, Kapaniris O, Slavotinek A, Betts WH, Ward AD, Lincoln SF, Mahadevan I.** Video image analysis of labile zinc in viable pancreatic islet cells using a specific fluorescent probe for zinc. *J Histochem Cytochem* 42: 877–884, 1994.